Bulk viscosity of the Lennard-Jones system at the triple point by dynamical nonequilibrium molecular dynamics

Pier Luca Palla,[1,*] Carlo Pierleoni,[2,†] and Giovanni Ciccotti[3,‡]

[1]*Department of Physics, and Sardinian Laboratory for Computational Materials Science (SLACS, INFM-CNR), University of Cagliari, Cittadella Universitaria, I-09042 Monserrato (Ca), Italy*

[2]*CNISM and Dipartimento di Fisica, Università de L'Aquila, I-67100 L'Aquila, Italy*

[3]*CNISM and Dipartimento di Fisica, Università di Roma "La Sapienza", Centro Interdisciplinare Linceo "B. Segre", Accademia dei Lincei, Roma, Italy*

(Received 31 March 2008; published 29 August 2008)

Nonequilibrium molecular dynamics (NEMD) calculations of the bulk viscosity of the triple point Lennard-Jones fluid are performed with the aim of investigating the origin of the observed disagreement between Green-Kubo estimates and previous NEMD data. We show that a careful application of the Doll's perturbation field, the dynamical NEMD method, the instantaneous form of the perturbation and the "subtraction technique" provides a NEMD estimate of the bulk viscosity at zero field in full agreement with the value obtained by the Green-Kubo formula. As previously reported for the shear viscosity, we find that the bulk viscosity exhibits a large linear regime with the field intensity.

DOI: 10.1103/PhysRevE.78.021204 PACS number(s): 66.20.Cy, 66.20.Ej, 83.10.Rs

I. INTRODUCTION

The calculation of the hydrodynamics transport coefficients for model systems is a noticeable success of molecular dynamics (MD) [1]. The standard method to compute linear transport coefficients by molecular dynamics simulations makes use of the Green-Kubo formulas [2–4]. Based on the dissipation-fluctuation theorem, Green-Kubo formulas allow us to compute linear transport coefficients from dynamical fluctuations of suitably defined microscopic currents at equilibrium. The Green-Kubo methodology can be easily implemented in a simulation of the equilibrium state and all transport coefficients can be obtained in the same calculations.

An alternative approach to the computation of transport coefficients is to mimic the appropriate nonequilibrium state. This can be generally obtained by applying a suitable external force and measuring the response related to the corresponding transport coefficient. Nonequilibrium molecular dynamics (NEMD) has been developed along these lines already in the early 1980s. It was soon realized that some paradigms of equilibrium molecular dynamics (EMD) had to be relaxed to mimic nonequilibrium processes. In particular, the use of periodic boundary conditions (PBC), a key ingredient of EMD to minimize finite size effects, is often incompatible with the nonequilibrium state of interest. In many interesting cases the external field acts through the boundaries, for instance, a thermal gradient or a velocity gradient, and the simulation of such a system can require abandoning the use of PBC in favor of less convenient boundaries. This was, for instance, the case of a system under the action of a thermal gradient [5,6] or in a Poiseuille flow [7]. Nonperiodic boundaries however require quite large systems which had limited the early use of direct nonequilibrium methods. To circumvent these limitations the so-called "synthetic" NEMD algorithms have been developed and extensively used in the exploration of nonequilibrium phenomena [8]. The general idea behind this class of algorithms is to replace the external force by an effective, PBC compatible, bulk field which, in the limit of vanishing intensity, excites the same response as the original external force. In this way the linear regime can, in principle, be explored without abandoning the use of PBC and therefore avoiding large finite size effects. In the case of fluid flows this technique requires the use of periodic but moving boundary conditions [8,9]. It should be noted that, after restoring the use of PBC, the heat produced by the external bulk field must be removed by a "bulk" thermostatting mechanism such as, for instance, a Nose-Hoover thermostat. We want to emphasize that the theoretical foundation of this class of algorithm is the linear response theory and their use beyond the linear regime is somewhat arbitrary. In this context the "subtraction technique" [11,12] is a very useful tool (at least for simple systems in which the response time is not longer than the typical Lyapunov time) to perform the vanishing perturbation limit. For almost all transport coefficients a good agreement between GK method and synthetic NEMD methods has been found [13–19]. The bulk viscosity makes a noticeable exception. In Fig. 1 we show the results of several computations of the bulk viscosity of a Lennard-Jones fluid close to the triple point. Most of these works adopted the Green-Kubo method [20–25] and found very similar results. Only two NEMD calculations have been performed so far [10,26] and they both provide values of the bulk viscosity 30–50% higher than the Green-Kubo values. Note that finite size effects cannot explain the observed discrepancies.

In the present work we reconsider the calculation of the bulk viscosity of the Lennard-Jones fluid close to the triple point and show that a careful application of the well-known Doll's synthetic algorithm provides estimates of the bulk viscosity in full agreement with the Green-Kubo values. The paper is organized as follows. In Sec. II we provide the nec-

*pierluca.palla@dsf.unica.it

†Carlo.Pierleoni@aquila.infn.it

‡giovanni.ciccotti@roma1.infn.it

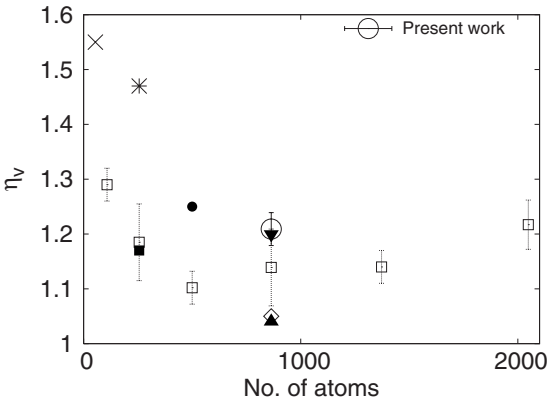

FIG. 1. Review of previous results for the bulk viscosity of a simple Lennard-Jones fluid close to the triple point versus the system size. The NEMD data are from Ref. [26] (×) and Ref. [10] (∗), while the EMD are from Ref. [20] (□), Ref. [21] (◇), Ref. [22] (▼), Ref. [23] (●), Ref. [24] (■), and Ref. [25] (▲). The viscosity is expressed in Lennard-Jones natural units.

essary theoretical background by discussing both the Green-Kubo formula for the bulk viscosity coefficient and the dynamical NEMD approach we have adopted. Section III deals with details of the simulation such as the time dependence of the perturbation, the simulation box, and the implementation of the dynamical approach to NEMD. In Sec. IV we collect our results and in Sec. V we provide some concluding remarks. In the Appendix we show that, in the linear regime, the synthetic perturbation for the viscosity is, as generally assumed, proportional to the velocity field produced.

II. THEORETICAL BACKGROUND

A. Hydrodynamics and microscopic identification of local fields

The bulk viscosity is one of the transport coefficients introduced in hydrodynamics [4]. In this theory, the fluid is described by classical fields which, in the case of a simple neutral system, are the mass, momentum and energy density fields. Partial differential equations derived from the continuity equation, supplemented by the so-called "constitutive relations" and by the local equilibrium hypothesis, provide a closed theoretical framework for the evolution of these fields. The "constitutive relations" are linear relations between the external forces acting on the system and the excited flows, the coefficients being the transport coefficients specific for each material. The viscosity coefficients, namely the bulk viscosity, η_v, and the shear viscosity, η_s, are defined by the Newton constitutive law

$$\underline{\underline{P}}(\vec{r},t) = \left[\bar{p}(\vec{r},t) - \left(\eta_v - \frac{2}{3}\eta_s\right)\vec{\nabla}\cdot\vec{v}(\vec{r},t)\right]\underline{\underline{I}} - \eta_s\{\vec{\nabla}\vec{v}(\vec{r},t) + [\vec{\nabla}\vec{v}(\vec{r},t)]^{\dagger}\}, \quad (1)$$

where $\underline{\underline{P}}$ is the pressure tensor, $\vec{v}$ the velocity field, and $\underline{\underline{I}}$ the identity tensor. $\bar{p}$ represents the hydrostatic pressure, which, according to the local equilibrium hypothesis, can be expressed in terms of the mass density, $m(\vec{r},t)=mn(\vec{r},t)$, and the energy density, $e(\vec{r},t)$, by the equilibrium equation of state

$$\bar{p}(\vec{r},t) = P_{eq}[mn(\vec{r},t), e(\vec{r},t)], \quad (2)$$

where $n(\vec{r},t)$ is the local number density. If the velocity field reduces to the particular form $\vec{v}(\vec{r},t)=\vec{r}f(t)$, with $f(t)$ a yet unspecified function of time, the Newton law reduces to

$$\frac{1}{3}\mathrm{Tr}[\underline{\underline{P}} - \bar{p}\underline{\underline{I}}] = -3\eta_v f(t), \quad (3)$$

where the symbol Tr stands for the trace of the tensor.

According to Irving and Kirkwood [27], any macroscopic hydrodynamic field $J(\vec{r},t)$ can be obtained from the statistical average, over the time dependent ensemble, $\rho(\Gamma,t)$, of a microscopic observable $\hat{J}(\Gamma)$, where $\Gamma=\{\vec{r}_i,\vec{p}_i\}$ $(i=1,N)$ is the phase-space point of the N particles system. In the specific case of the pressure tensor we have [4]

$$\underline{\underline{P}}(\vec{r},t) = \left\langle \sum_{i=1}^{N} \delta(\vec{r}-\vec{r}_i)\left[\frac{\vec{p}_i\vec{p}_i}{m} + \vec{r}_i\vec{F}_i\right] \middle| \rho(\Gamma,t)\right\rangle, \quad (4)$$

where $\vec{F}_i$ is the internal force acting on particle i. The number and energy densities can also be expressed as

$$n(\vec{r},t) = \left\langle \sum_{i=1}^{N} \delta(\vec{r}-\vec{r}_i) \middle| \rho(\Gamma,t)\right\rangle \quad (5)$$

$$e(\vec{r},t) = \left\langle \sum_{i=1}^{N} \delta(\vec{r}-\vec{r}_i)\left[\frac{|\vec{p}_i|^2}{2m} + \frac{1}{2}\sum_{j\neq i}\phi(r_{ij})\right] \middle| \rho(\Gamma,t)\right\rangle, \quad (6)$$

where $\phi(r)$ represents the pair potential of our model system. The local hydrostatic pressure $\bar{p}(\vec{r},t)$ is the trace of the pressure tensor and, within the local equilibrium hypothesis, its fluctuations around the equilibrium value $p_0(n_0,e_0)$ can be expressed as

$$\bar{p}(\vec{r},t) = p_0 + \left.\frac{\partial P_{eq}}{\partial e}\right|_{e_0}[e(\vec{r},t)-e_0] + \left.\frac{\partial P_{eq}}{\partial n}\right|_{n_0}[n(\vec{r},t)-n_0]. \quad (7)$$

The bulk viscosity coefficient in terms of statistical averages is then obtained, for velocity fields of the form prescribed above, by replacing the fields in Eq. (3) with the appropriate dynamical ensemble averages. Furthermore, in order to ensure the validity of local equilibrium, it is required to take the "hydrodynamic limit:"

$$\eta_v = -\lim_{\omega\to 0}\lim_{k\to 0}\frac{\mathrm{Tr}[\underline{\underline{\tilde{P}}}(\vec{k},\omega) - \tilde{\bar{p}}(\vec{k},\omega)\underline{\underline{I}}]}{9\tilde{f}(\omega)}, \quad (8)$$

where $\tilde{J}(\vec{k},\omega)=\frac{1}{V}\int\int d\vec{r}dt\,\exp(i\vec{k}\cdot\vec{r})\exp(i\omega t)J(\vec{r},t)$ is the usual Fourier transform (in space and in time) of the field.

B. Green-Kubo formula

Equation (8) expresses the bulk viscosity as an average on the nonequilibrium distribution $\rho(\Gamma,t)$. When the system is

close to equilibrium (linear hydrodynamics) it is possible to rewrite it by the Green-Kubo formula [28,29]:

$$\eta_v = \beta V \int_0^{+\infty} dt \langle \hat{J}(t)\hat{J}(0)\rangle_0, \tag{9}$$

with

$$\hat{J}(t) = [\hat{\mathcal{P}}(t) - \langle \hat{\mathcal{P}} \rangle] - \frac{1}{V}\left\{ \left. \frac{\partial P_{eq}}{\partial e} \right|_n [\hat{\mathcal{H}}(t) - \langle \hat{\mathcal{H}} \rangle] \right\}, \tag{10}$$

where V, e are the volume and internal energy per unit volume of the system, respectively. $\hat{\mathcal{P}}$ and $\hat{\mathcal{H}}$ are the dynamical variables corresponding to the thermodynamic pressure and energy

$$\hat{\mathcal{P}}(t) = \lim_{k\to 0} \frac{1}{3V} \mathrm{Tr}(\tilde{\underline{\underline{\hat{P}}}}(\vec{k},t)) = \frac{1}{3V} \sum_{i=1}^{N} \mathrm{Tr}\left[\frac{\vec{p}_i \vec{p}_i}{m} + \vec{r}_i \vec{F}_i \right], \tag{11}$$

$$\hat{\mathcal{H}}(t) = \lim_{k\to 0} \tilde{\hat{e}}(\vec{k},t) = \sum_{i=1}^{N} \left[\frac{|\vec{p}_i|^2}{2m} + \frac{1}{2} \sum_{j\neq i} \phi(r_{ij}) \right]. \tag{12}$$

Equation (10) is the general expression of the current related to the bulk viscosity coefficients in the general case in which the energy fluctuates. If experiments are conducted in the microcanonic ensemble the energy fluctuations vanish and the more familiar expression of the Green-Kubo formula is obtained [4].

C. "Doll's" perturbation and the "dynamical approach" to nonequilibrium molecular dynamics

As described in the introduction, the alternative route to transport properties is to consider the system subjected to an external perturbation able to mimic the "thermodynamic force" which excites the appropriate nonequilibrium flux inside the system. In the present case the "thermodynamic force" is the macroscopic velocity gradient, $\vec{\nabla}\vec{v}$, while the corresponding flux is the deviation of the pressure from its local equilibrium value, $\frac{1}{3}\mathrm{Tr}[\underline{\underline{P}}] - \bar{p}$. The bulk external force to be used in such experiments is known as "Doll's" perturbation:

$$\hat{H}'(\Gamma,t) = \sum_{i}^{N} \vec{r}_i \vec{p}_i : [\vec{\nabla}\vec{u}(\vec{r}_i,t)]^T, \tag{13}$$

where $\vec{\nabla}\vec{u}(\vec{r},t)$ is the required external field. This perturbation was proposed by Luttinger [30] and adopted in a molecular dynamics simulation by Hoover *et al.* [26,32]. In the Appendix we will show that, in the linear regime, the macroscopic velocity field $\vec{v}(\vec{r},t)$ induced by this perturbation coincides with the imposed external constraint $\vec{u}(\vec{r},t)$ in the long wavelength limit

$$\tilde{\vec{v}}(\vec{k}=0,\omega) = \tilde{\vec{u}}(\vec{k}=0,\omega). \tag{14}$$

Once we are able to induce the required hydrodynamic flux, we need a procedure to compute the average of the response on the nonequilibrium ensemble.

To this aim we can exploit the "Onsager-Kubo" relation [11,12,31]. Calling $S(t)$ the time evolution operator of the perturbed dynamics, the following relation holds for the nonequilibrium average of the generic microscopic flux $\hat{J}$:

$$\begin{aligned} \langle \hat{J} \rangle_t &\equiv \int \hat{J}(\Gamma)\rho(\Gamma,t)d\Gamma \\ &= \int \hat{J}(\Gamma) S^{\dagger}(t)\rho_0(\Gamma)d\Gamma = \int S(t)J(\Gamma)\rho_0(\Gamma)d\Gamma \\ &= \int \hat{J}(t)\rho_0(\Gamma)d\Gamma \equiv \langle \hat{J}(t)\rangle_0, \end{aligned} \tag{15}$$

where $S^{\dagger}(t)$ is the adjoint of $S(t)$ and $\rho_0(\Gamma)$ is the ensemble distribution at the time $t=0$. If the perturbation is switched on at time $t=0$ from an equilibrium state, ρ_0 is the equilibrium distribution and the Onsager-Kubo relation (15) allows us to compute the required average in a rigorous way. Indeed, via standard equilibrium MD simulation, we can obtain a set of statistically independent configurations $\{\Gamma_i\}$ distributed according to $\rho_0(\Gamma)$. Starting from those configurations we can follow the evolution of the system under the perturbed dynamics and obtain the required nonequilibrium average as the average of the evolved observable over the initial distribution according to the Onsager-Kubo relation.

When a large perturbation is applied, a thermostatting mechanism needs to be added to the equation of motion and the response can depend on it. Conversely, for vanishingly small perturbations the standard form of linear response theory [3,4] holds and the response depends only on the applied perturbation. In this limit, however, an additional numerical problem is encountered. The fluctuations of the microscopic variables are quite large and dominate the response in the limit of vanishing perturbations. In simple systems, where the response time is comparable to the Lyapunov time of the exponential divergence of nearby starting trajectories, the "subtraction technique" can be used to extract the signal out of the statistical noise [11,12]. If $S_0(t)$ is the evolution operator representing the unperturbed dynamics with $\langle S_0(t)\hat{J}\rangle_0 = 0$, the average values $\langle S(t)\hat{J} - S_0(t)\hat{J}\rangle_0$ and $\langle S(t)\hat{J}\rangle_0$ are equal. On the other hand, their variances are very different: the thermal fluctuations of $S(t)\hat{J}$ and $S_0(t)\hat{J}$ are highly correlated and therefore largely cancel each other. This is true for times short enough. At large times the variance of the difference estimator becomes twice the variance of the simple estimator.

III. SIMULATION TECHNIQUE

A. Impulsive external field

As mentioned above, the current associated to the bulk viscosity to be used both in the Green-Kubo formula or in the NEMD experiments depends on the statistical ensemble chosen to conduct the experiment. In all previous equilibrium calculations, as well as in the present one, the microcanonical ensemble was chosen since the current reduces to the pressure tensor fluctuations without the need of evaluating the additional term related to the energy fluctuations.

In NEMD, the Doll's perturbation for the bulk viscosity is a pure contraction or expansion of the volume so that a constant perturbation in time, $f(t)=\epsilon$, will correspond to an exponential contraction/expansion of the volume (see next subsection), obviously an impractical way to extract the bulk viscosity coefficient. Alternative forms of $f(t)$ can be an oscillating function $f(t)=\epsilon \sin(t)$ and an impulsive perturbation $f(t)=\epsilon\delta(t)$, where ϵ is the intensity of the field. The oscillating form, used in previous NEMD calculations, requires thermostatting the nonequilibrium trajectory in order to reach a steady state and the extended form of the current with the energy fluctuation term must be used. On the other hand, the impulsive perturbation acts on the system for an infinitesimal time, no thermostatting mechanism is necessary, and the dynamics after the impulse is the equilibrium dynamics for the isolated system. This fact greatly simplifies the NEMD experiment and the form of the flux, Eq. (10). For each initial configuration Γ_i, the energy and the volume of the system change from their initial values $\mathcal{H}_0$ and V_0 of the equilibrium system, to the time independent values $\mathcal{H}_i'=\hat{\mathcal{H}}_i(t>0^+)$ and $V'=\hat{V}(t>0^+)$ (note that all replicas undergo the same volume change). In order to obtain the appropriate flux in Eq. (10) we have to calculate only the dynamical variable $\hat{\mathcal{P}}(t)$ and its average asymptotic value:

$$p_\infty = \lim_{t\to\infty}\langle\hat{\mathcal{P}}\rangle_t, \tag{16}$$

where $\langle\cdots\rangle_t$ are averages over the nonequilibrium distribution at time t. Note that p_∞ is not a properly defined pressure because the corresponding ensemble is not well-defined since each member of the ensemble has a different energy. It is rather the asymptotic large time value of $\langle\hat{\mathcal{P}}\rangle_t$ that needs to be subtracted to it in order to make the current integrable in time to provide the associated transport coefficient.

B. Periodic boundary conditions

The explicit form of the Doll's perturbation field with a homogeneous velocity gradient $\nabla u=f(t)\mathbb{I}$, is not compatible with the periodic boundary conditions of MD. However the periodicity of the system can be restored if we allow the box matrix $\underline{\underline{H}}$ to evolve according to the external flow [33]

$$\dot{\underline{\underline{H}}}(t) = \underline{\underline{\nabla u}}\cdot\underline{\underline{H}}(t). \tag{17}$$

Starting with a cubic cell of edge $L_\alpha(0)=L_0(\{\alpha=x,y,z\})$, and applying a velocity field $\nabla u=\epsilon\delta(t)\mathbb{I}$ we get

$$L_\alpha(t\geqslant 0^+) = L_0 e^{\epsilon} \simeq L_0(1+\epsilon). \tag{18}$$

Similarly, the perturbation induces a discontinuity in the trajectory of the system

$$\dot{\vec{r}}_i = \frac{\vec{p}_i}{m} + \epsilon\delta(t)\vec{r}_i, \quad \dot{\vec{p}}_i = \vec{F}_i - \epsilon\delta(t)\vec{p}_i \tag{19}$$

which correspond to

$$\vec{r}_i(0^+) = \vec{r}_i(0^-)e^{\epsilon} \simeq \vec{r}_i(0^-)(1+\epsilon),$$

$$\vec{p}_i(0^+) = \vec{p}_i(0^-)e^{-\epsilon} \simeq \vec{p}_i(0^-)(1-\epsilon). \tag{20}$$

Therefore, the effect of the impulsive perturbation is to apply a homogeneous contraction (expansion) of the position space and a homogeneous expansion (contraction) in the momentum space of the system. Substituting Eqs. (20) in the perturbed Hamiltonian $\hat{\mathcal{H}}(0^+)=\hat{\mathcal{H}}_0+\epsilon\Sigma_i\vec{r}_i(0^+)\cdot\vec{p}_i(0^+)$ and using Eq. (11), the variation of energy induced by the impulsive field is

$$\hat{\mathcal{H}}(0^+) - \hat{\mathcal{H}}(0^-) = -\hat{\mathcal{P}}(0^-)dV + \mathcal{O}(\epsilon^2),$$

where V is the volume of the system. Taking the ensemble average over the equilibrium distribution at $t=0^-$, we recover the first principle of thermodynamics

$$\Delta E = -pdV. \tag{21}$$

C. Bulk viscosity computation

With the impulsive field of previous section, Eq. (8) for the bulk viscosity reduces to

$$\eta_v = \lim_{\omega\to 0}\lim_{k\to 0} -\frac{\frac{1}{3}\mathrm{Tr}[\underline{\underline{\tilde{P}}} - \tilde{\tilde{p}}\underline{\underline{I}}]}{\mathrm{Tr}(\underline{\underline{\tilde{\nabla}}}\tilde{\vec{v}})} = \lim_{\epsilon\to 0} -\frac{1}{3\epsilon}\int_0^\infty [\langle\hat{\mathcal{P}}\rangle_t - p_\infty]dt. \tag{22}$$

Using the Onsager-Kubo relation to rewrite nonequilibrium ensemble averages in terms of equilibrium averages of evolved observables, and applying the subtraction technique described above, we obtain

$$\eta_v = \lim_{\epsilon\to 0} -\frac{1}{3\epsilon}\int_0^\infty \{[\langle S(t)\hat{\mathcal{P}} - S_0(t)\hat{\mathcal{P}}\rangle_0] - [p_\infty - p_0]\}dt, \tag{23}$$

where $S(t)$ and $S_0(t)$ are the evolution operators for the perturbed and equilibrium dynamics respectively. Note that $p_0=P_{eq}(\hat{\mathcal{H}}_0,n_0)$ is the pressure of the equilibrium microcanonical system, while as mentioned above, p_∞ is not a properly defined averaged pressure.

D. Simulations scheme and numerical details

As already mentioned, the operative procedure to compute Eq. (23) is to select a set of statistically uncorrelated equilibrium configurations of the system $\{\Gamma_i\}$, for each member of the set to generate both the equilibrium and the nonequilibrium evolutions, and to compute the term $[\langle S(t)\hat{\mathcal{P}} - S_0(t)\hat{\mathcal{P}}\rangle_0]$ up to a time t_r, as the arithmetic mean over the set. The time t_r is the typical time the individual nonequilibrium system C_i of energy $\hat{\mathcal{H}}_i(0^+)$ takes to relax from the perturbed initial configuration to its equilibrium state. The additional offset term, involving p_∞, is the stationary value of that average beyond t_r. In order to reduce the statistical noise

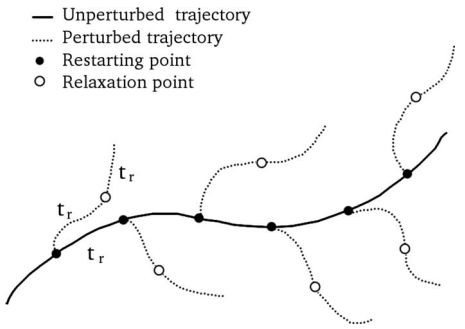

FIG. 2. Simulations scheme: a long unperturbed trajectory of the system is used to sample initial conditions for segment of perturbed trajectories. Each integration of the perturbed equations of motion has been integrated for twice the estimated signal relaxation time. This is needed to evaluate the thermodynamic pressure of the segments.

on this term we have computed, for each individual nonequilibrium trajectory, the time average of the microscopic "pressure" between t_r and $2t_r$, and we have estimated the offset as the arithmetic mean of those time averages over all nonequilibrium trajectories.

The system considered in this work is a simple fluid of $N=864$ particles interacting by the Lennard-Jones potential, in a thermodynamic state close to the triple point. In the following all quantities will be expressed in Lennard-Jones units: $\epsilon=1$, $\sigma=1$, $m=1$. The potential has been truncated at $r_{cut}=2.5$ and shifted to avoid discontinuity at r_c. Moreover, for $r\in[2.4:2.6]$ the potential has been replaced with a cubic polynomial in order to avoid discontinuities in the forces at the cutoff. The equations of motion have been integrated through a velocity Verlet algorithm with an integration step $h=0.004\,436$.

The unperturbed trajectory (see Fig. 2) has been integrated for 9.9×10^6 integration steps. No thermalizing device is added to the equilibrium dynamics so that a sampling of the microcanonical ensemble is obtained. This equilibrium trajectory was used to compute the bulk viscosity through the Green-Kubo formula. The time of saturation of the Green-Kubo integral, i.e., the decorrelation time of the pressure fluctuations at equilibrium, has been used as an estimate of the relaxation time t_r. The set of initial equilibrium configurations are therefore selected as equilibrium configurations a time t_r apart from each other along the equilibrium trajectory. In order to calculate the response of the system to the impulsive external field, $S(t)\hat{\mathcal{P}}$, the perturbed trajectories have been integrated for a time t_r and extended to $2t_r$ in order to evaluate the offset term (see Fig. 2).

TABLE I. Thermodynamic equilibrium state. The simulated system is in a state very close to that used in most of previous MD studies of the bulk viscosity.

Density	(Energy)/N	Temp.	Pressure
0.8442	−4.112561(5)	0.72111(4)	0.8978(3)

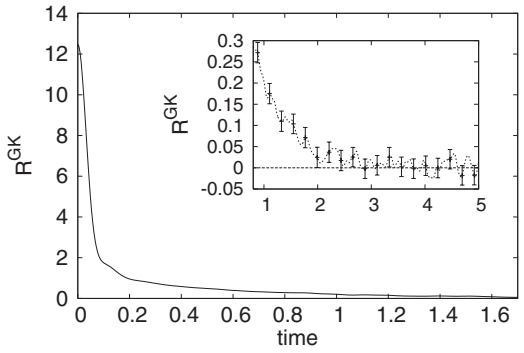

FIG. 3. Green-Kubo integrand [see Eq. (9)]. In the inset we show an enlargement of the tail.

IV. RESULTS

The thermodynamic state of the equilibrium system is reported in Table I. This state is very close to that used in previous studies [10,20–26].

A. Green-Kubo results

In Fig. 3 we report the Green-Kubo integrand $R^{GK}(t)=\beta V\langle\hat{\mathcal{P}}(t)\hat{\mathcal{P}}(0)\rangle_0$. After a rapid relaxation in about 0.22 time units, the curve exhibits a long time tail which vanishes only beyond $t=2$ (see the inset). Although the noise level on the time correlation function is quite small, the noise on its time integral, as obtained by a simple trapezoidal rule, results in being quite large because of the long tail. In order to get a smoothed signal we have attempted to replace the data beyond $t=0.22$ with two different analytic functions, fitted to the data in the time interval [0.22:2.0]. We have assumed a power law behavior $R_v^{GK}(t)\sim at^{-b}$ and an exponential behavior $R^{GK}(t)\sim ae^{-bt}$ (the power law behavior is compatible with Hoover's hypothesis [26]: $\eta_v^{GK}(\omega)=a'+b'\sqrt{\omega}$, i.e., $R^{GK}(t)\sim t^{-3/2}$). Values of the fitting parameters are reported in Table II while the data and the fitting functions are compared in Fig. 4.

From Table II and Fig. 4, we conclude that the exponential behavior is a better representation of our data. Integration of the correlation function supplemented by our best exponential fit provides the behavior in Fig. 5 and the following value for the viscosity

$$\eta_v^{GK}=1.22\pm0.03.$$

B. NEMD results

In Table III we report the details and thermodynamic results from the performed nonequilibrium experiments. Note

TABLE II. Fitting parameters for the tail of the Green-Kubo integral.

	Fitting interval	a	b	χ^2/ndf
$\eta=at^b$	$t\in[0.22:2.0]$	0.0160(2)	−1.09(1)	1×10^{-5}
$\eta=ae^{-bt}$	$t\in[0.22:2.0]$	0.1004(6)	1.83(1)	2×10^{-6}

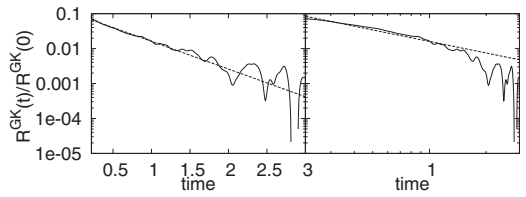

FIG. 4. Tail of the Green-Kubo integrand $R^{GK}(t)$ and its fitting functions. Data are normalized by the initial value $R^{GK}(0)$. The fitting range is $t \in [0.22:2]$. In the left panel we show (in linear-log scale) the exponential fit, while in the right panel we show (in log-log scale) the power law fit.

that positive ϵ corresponds to nearly adiabatically expanded systems and therefore to reduced temperatures (remember that the systems remain isolated after the impulsive external perturbation at $t=0$). In the second to last column, we report the average variation of the total energy ΔE due to the impulsive perturbation. Comparing the data in the last two columns, we can verify the validity of Eq. (21) in the limit of small ϵ ($|\epsilon| < 0.002$). In order to analyze the response of the system, we need to separately discuss the various contributions to the integrand in Eq. (23). For the sake of clarity, let us define the following quantities:

$$\Delta(t) = \frac{\langle [S(t)\hat{\mathcal{P}} - S_0(t)\hat{\mathcal{P}}] \rangle_0}{-3\epsilon}, \tag{24}$$

$$\Delta^{\infty} = \frac{p_{\infty} - p_0}{-3\epsilon}, \tag{25}$$

$$R(t,\epsilon) = \Delta(t) - \Delta^{\infty}, \tag{26}$$

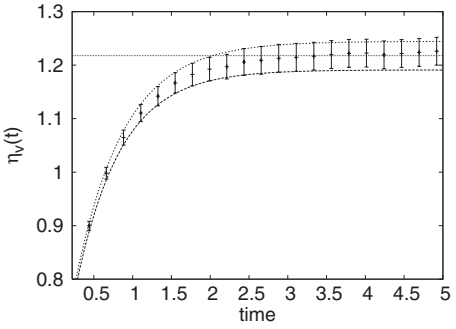

FIG. 5. Green-Kubo integral: $\eta_v(t) = \int_0^t ds R^{GK}(s)$. The horizontal plateau value is our Green-Kubo estimate of the bulk viscosity coefficient.

$$\eta_v(t,\epsilon) = \int_0^t ds R(s,\epsilon). \tag{27}$$

The newtonian bulk viscosity is the zero field-infinite time limit of $\eta_v(t,\epsilon)$. In Table IV and Fig. 6, we report data for $\Delta(0)$ and Δ^{∞} defined in Eqs. (24) and (25).

We note that the error on Δ^{∞} grows when $|\epsilon|$ decreases while the error on $\Delta(0)$ remains roughly constant. This is the effect of the subtraction technique that improves the signal to noise ratio for short t only while it has no effect at large time where Δ^{∞} has to be calculated. A less noisy estimate of Δ^{∞} for $|\epsilon| < 0.002$ can be obtained by linear interpolation of the less noisy data at larger absolute values of the perturbation (see Fig. 6).

In Fig. 7 we show the values of the integrand in Eq. (23) at $t=0^+$, i.e., $R(0) = \Delta(0) - \Delta^{\infty}$. At $\epsilon=0$ we display $R^{GK}(0)$. As predicted by linear response theory, we observe that the NEMD response tends to the quadratic fluctuations of the pressure at equilibrium in the limit $|\epsilon| \to 0$.

In Fig. 8 we show the estimates of the $\eta_v(t,\epsilon)$ curves. We note that, as $|\epsilon|$ decreases, the noise level at large time in-

TABLE III. Thermodynamic properties of the system subjected to the external perturbation. As for the p_{∞}, the values of the temperature T and of the energy variation ΔE are obtained as the arithmetic mean of the corresponding properties over all nonequilibrium trajectories, see Sec. III D. By comparing the data in the last two columns, we can verify the validity of Eq. (21). As explained in Sec. III B, this equation states the consistency of the "Doll's" perturbation with the first principle of thermodynamics.

ϵ	N_{seg}	N/V	T	$\Delta E/N$	$-p_0 dV/N$
0.05	9000	0.7292	0.5408(2)	0.2191(1)	0.2023(2)
0.02	9000	0.7955	0.6174(2)	0.01049(6)	0.02648(6)
0.005	13000	0.8317	0.6912(1)	−0.01080(2)	−0.02160(1)
0.002	16400	0.8392	0.70892(9)	−0.005538(5)	−0.006386(5)
5×10^{-4}	16500	0.8429	0.71726(8)	−0.001539(1)	−0.001511(2)
2×10^{-4}	16500	0.8437	0.71909(9)	$-6.284(5)\times10^{-4}$	$-6.263(5)\times10^{-4}$
0		0.8442	0.72111(4)		
-2×10^{-4}	12000	0.8447	0.7220(1)	$6.432(6)\times10^{-4}$	$6.352(5)\times10^{-4}$
-5×10^{-4}	16500	0.8455	0.72335(9)	0.001645(1)	0.001660(1)
−0.002	16400	0.8493	0.7338(1)	0.007222(5)	0.006360(5)
−0.005	13000	0.8570	0.7533(1)	0.02133(2)	0.01585(1)
−0.02	9000	0.8969	0.86865(2)	0.1603(1)	0.06218(7)
−0.05	9000	0.9846	1.1894(5)	0.9154(3)	0.6539(5)

TABLE IV. In the second and in the third column we report the data for $\Delta(0)$ and Δ^{∞}, respectively [see Eqs. (24) and (25)] while, in the last column, the bulk viscosity for the corresponding intensity of the perturbation is shown. The time interval used for fitting the exponential function to the data is also reported in the second to last column.

ϵ	$\Delta(0)$	Δ^{∞}	Range for the fit	η_v
0.05	25.132(5)	13.757(6)	0.44:2.66(500 pts)	3.77(2)
0.02	32.884(5)	21.382(7)	0.44:2.66(500 pts)	1.39(2)
0.005	37.778(4)	25.61(2)	0.44:2.66(500 pts)	1.25(6)
0.002	38.863(4)	26.53(4)	0.44:2.22(400 pts)	1.2(1)
0.0005	39.415(4)	27.1(2)	0.22:1.22(230 pts)	1.15(6)
0.0002	39.527(4)	26.6(4)	0.22:1.22(230 pts)	1.15(6)
0(GK)				1.22(3)
−0.0002	39.663(5)	26.9(5)	0.22:1.22(230 pts)	1.13(6)
−0.0005	39.787(4)	27.2(2)	0.22:1.22(230 pts)	1.15(6)
−0.002	40.351(4)	27.80(4)	0.44:2.22(400 pts)	1.2(1)
−0.005	41.499(5)	28.74(2)	0.44:2.66(500 pts)	1.18(5)
−0.02	47.888(6)	34.116(7)	0.44:2.66(500 pts)	1.13(2)
−0.05	64.387(8)	47.770(5)	0.44:2.66(500 pts)	1.15(2)

creases considerably. This signals again the limit of applicability of the subtraction technique. Similar to the Green-Kubo case of the previous section, a less noisy estimator of the viscosity is obtained by integrating a response function in which the long time tail is replaced by an exponentially decaying behavior fitted to the data at large time.

Finally, in Table IV and Fig. 9 we report the values of $\eta_v(\epsilon)=\lim_{t\to\infty}\eta_v(t,\epsilon)$. As expected the data in the small ϵ region ($|\epsilon|\leqslant 0.005$) are in agreement with the Green-Kubo estimate of the viscosity. Although equilibrium and NEMD data are in agreement within error bars, $\eta_v(\epsilon)$ data for $|\epsilon|\leqslant 0.005$ exhibit an unexpected small error bar and appear to be systematically below the Green-Kubo prediction. This is probably a small bias of our extrapolation procedure. The large noise in the tail of the response function forces us to perform the fit in a time interval considerably smaller than for larger perturbations (see Table IV). This might lead to underestimated errors (see Fig. 8) and to an estimate of the asymptotic value slightly lower than the correct value.

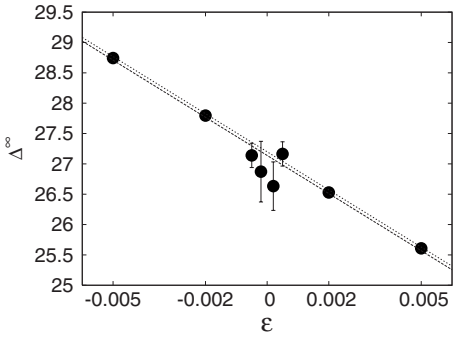

FIG. 6. Trend of the offset, Δ^{∞}, defined in Eq. (25), as a function of the applied deformation ϵ. For $|\epsilon|<0.002$ the values are affected by a large error. An interpolation of the other data is used to reduce the noise in this region.

C. Nonlinear regime

The results of the previous section show the consistency between Green-Kubo and NEMD estimates of the bulk viscosity coefficient. However at variance with other coefficients, such as, for instance, the shear viscosity, where a linear regime over several orders of magnitude of the intensity of the external perturbation is observed (up to roughly 0.05) [35], in the present case the linear regime is apparently much reduced. This can be clearly seen in Fig. 7 where the NEMD results for $R(0^+,\epsilon)$ matches the GK value with a finite slope suggesting that a linear expansion of the response function with the perturbation field is never justified. The same effect is seen for the viscosity in Fig. 9 (see the inset), although it is less pronounced and the much larger noise makes the observation less conclusive. In order to resolve this apparent paradox we must consider that the present perturbation, a contraction/expansion of the volume, excites the correct response and, at the same time, changes the thermodynamic state of the system. To correctly discuss the rheological nonlinear behavior of the fluid we should remove the

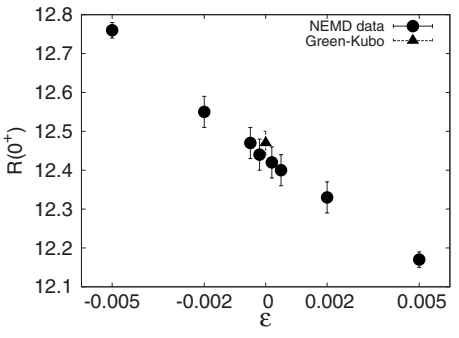

FIG. 7. Initial time response $R(0^+)$ versus the perturbation. NEMD data tends to the corresponding Green-Kubo value in the limit of small ϵ.

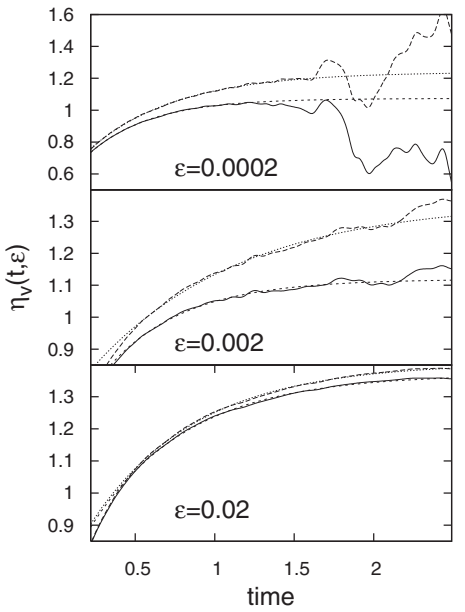

FIG. 8. Integral $\eta_v(t,\epsilon)$ of the response $R(t,\epsilon)$, see Eqs. (27), for some values of ϵ. At large time and for small values of $|\epsilon|$, the subtraction technique is not able to reduce the noise in the signal.

pure thermodynamic contribution to the response. Let us consider the viscosity as a function of the perturbation, the internal energy and the volume of the system: $\eta_v = \eta_v(\epsilon, e, V)$. In the present case of impulsive perturbation we have $V(0^+)=V_0[1+3\epsilon+O(\epsilon^2)]$, and $E(0^+)=E_0-p_0[V(0^+)-V_0]+O(\epsilon^2)=E_0-3\epsilon p_0 V_0+O(\epsilon^2)$ where E_0, V_0, and p_0 represent the energy, volume, and pressure of the equilibrium system respectively. The correct small ϵ expansion for the viscosity is therefore

$$\eta_v(\epsilon,e,V) = \eta_v + \left[\frac{\partial \eta_v}{\partial \epsilon} + 3V\left(\frac{\partial \eta_v}{\partial V} - p\frac{\partial \eta_v}{\partial E}\right)\right]_{\epsilon=0}\epsilon + O(\epsilon^2). \tag{28}$$

A similar expansion holds for $R(t)$, in particular for its value at $t=0^+$

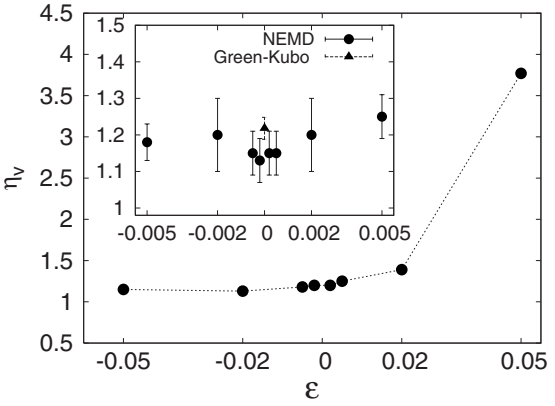

FIG. 9. Values of η_v calculated in the present work. In the inset we present a magnification of the small ϵ region. A good agreement with the Green-Kubo result is obtained.

TABLE V. Estimates of the thermodynamic derivatives in Eqs. (28) and (29) at the considered state point as obtained by the central difference formula.

$\partial\eta_v/\partial V=-0.0006(10)$	$\partial\eta_v/\partial E=-0.0024(8)$
$\partial R(0)/\partial V=-0.014(2)$	$\partial R(0)/\partial E=0.0021(9)$

$$R(0^+;\epsilon,e,V) = R(0^+)_{\epsilon=0} + \left[\frac{\partial R(0^+)}{\partial \epsilon} + 3V\left(\frac{\partial R(0^+)}{\partial V} - p\frac{\partial R(0^+)}{\partial E}\right)\right]_{\epsilon=0}\epsilon + O(\epsilon^2). \tag{29}$$

We have performed a series of EMD simulations at volumes and internal energies around the thermodynamic point studied and we have estimated the derivatives in equations (28) and (29) by the central difference formula. In Table V we report the estimated values of the derivatives. With those values the term in square brackets in Eq. (29) amounts to -50 ± 7 to be compared with -59 ± 2, the value of the estimated slope of the response in NEMD data (see Fig. 10). As for the viscosity itself, the value in the square brackets in Eq. (28) is 7 ± 2 to be compared with 6 ± 1, the estimated slope of the viscosity in Fig. 9. When data for $R(0^+)$ and η_v are corrected by these thermodynamic terms, a large linear regime appears, as reported in Figs. 10 and 11. This behavior confirms the simple LJ fluid as a true linear fluid in a large range of perturbations, the genuine rheological nonlinear behavior appearing only beyond $|\epsilon|\sim0.02$.

V. CONCLUSIONS

In the present paper we have reported nonequilibrium molecular dynamics calculations of the bulk viscosity of the Lennard-Jones fluid at triple point. Among the transport coefficients of the simple fluid, the bulk viscosity was the only one for which NEMD results, from two independent previous studies, did not agree with the Green-Kubo estimates (see Fig. 1). Surprisingly, this unexpected failure of the linear response theory remained unexplored for almost 25 years. In

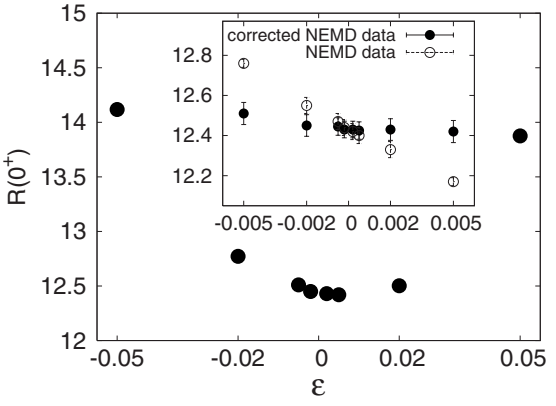

FIG. 10. Initial time response $R(0^+)$. The NEMD data are corrected by the thermodynamic term $3V(\frac{\partial R(0^+)}{\partial V}-p\frac{\partial R(0^+)}{\partial U})_{\epsilon=0}\epsilon$ [see Eq. (29)]. In the inset we show an enlargement of the small ϵ region.

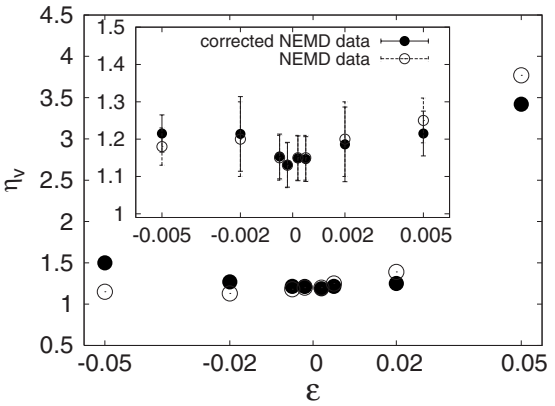

FIG. 11. Values of η_v^ϵ versus the perturbation. If the NEMD data are corrected by the thermodynamic term $3V(\frac{\partial \eta_v}{\partial V}-p\frac{\partial \eta_v}{\partial U})_{\epsilon=0}\epsilon$ [see Eq. (28)], then a large linear regime appears. In the inset we show an enlargement of the small ϵ region.

the present work we have resolved this apparent contradiction and found a full agreement between the NEMD and EMD estimates for the bulk viscosity.

We have applied the Doll's perturbation field to excite the relevant flux in the system. At variance with the shear or elongational viscosity cases where the external perturbation is a superposition of a rotation and a deformation of the system at constant volume [31,36], the field needed to excite the flux related to the bulk viscosity coefficient is a compression/expansion of the volume at constant shape. Such a perturbation excites the desired flux but also changes the thermodynamic state of the system. As a consequence, the relevant flux depends on the conditions at which the nonequilibrium experiment is conducted and, similarly, the Green-Kubo formula depends on the equilibrium ensemble used [29]. At equilibrium the microcanonical ensemble should be chosen to simplify the Green-Kubo analysis. As for the nonequilibrium experiments, two different techniques can be applied. One can apply the *stationary* NEMD method in which the system is driver toward a stationary nonequilibrium state by applying a periodic compression/expansion of the system. If the heat produced by the external field is removed by a thermostatting mechanism, the steady state can be maintained in time and the bulk viscosity can be estimated as the time average of the relevant flux divided by the perturbation strength. The other possible route is the *dynamical* NEMD in which a set of statistically uncorrelated replicas of the equilibrium system are subjected for $t \geqslant 0$ to the perturbation field and the evolution of the ensemble can be followed in time under the perturbed dynamics. The dynamical method is superior to the stationary method because not only steady state information can be obtained but also the transient behavior can be fully characterized. Moreover, within the *dynamical* NEMD, the *subtraction technique* can be used to perform the zero field strength limit and to extract the value of the linear transport coefficient. Another advantage of the dynamical method is that one can apply an impulsive perturbation rather than a periodic one. Since the system is perturbed for a very short period of time (one step of our discrete dynamics) we do not need to introduce a thermostatting mechanism to perform a meaningful experiment. Using dynamical NEMD with the subtraction technique and an impulsive form of the perturbation, we were able to explore a large range of perturbation strength and carefully study the small field regime. We have found a perfect agreement between the NEMD and the Green-Kubo estimates of the bulk viscosity. These estimates are also in agreement with previous values obtained by the Green-Kubo formula for various system sizes, while they do not agree with previous NEMD studies conducted by the stationary NEMD method. Finally, by removing the thermodynamic contribution to the viscosity, we show that the Lennard-Jones fluid at triple point exhibits a large linear regime, in agreement with the results for the shear viscosity [34].

APPENDIX: PERTURBATION ASSOCIATED TO VISCOUS FLUX: "DOLL'S"

In this section we will compute the response in the velocity field to the "Doll's" perturbation. By a straightforward application of the linear response theory we will find the result in Eq. (14). It proves that the "Doll's" perturbation is the perturbation producing every kind of viscous flux.

Let us consider a system of N particles of mass m with Hamiltonian of such a system will be

$$\hat{H}^{(0)} = \sum_{i=1}^{N} \frac{\vec{p}_i^2}{2m} + \sum_{j \neq i}^{N} \phi(|\vec{r}_{ij}|), \tag{A1}$$

where $\vec{r}_{ij}=\vec{r}_i-\vec{r}_j$ and $\phi(r)$ is the pair potential. We add a perturbation term of the form:

$$\hat{H}^{(I)}(\Gamma,t) = \int_V \underline{\underline{\alpha}}(\vec{r}):\underline{\underline{\Phi}}(\vec{r},t)d\vec{r}, \tag{A2}$$

where V is the volume of the system, $\underline{\underline{\alpha}}(\vec{r})$ is a local dynamical variable, and $\underline{\underline{\Phi}}(\vec{r},t)$ is the external field, dependent on time t and space $\vec{r}$. We assume that $\underline{\underline{\Phi}}$ is proportional to a small parameter ϵ defining the magnitude of the perturbation. The linear response theory states that the effect of $\hat{H}^{(I)}$ on a given observable $\hat{O}$ of the system is

$$O(\vec{r},t) = \langle \hat{O} \rangle_0 - \beta \int_0^\infty d\tau \int_V d\vec{s} \langle \hat{O}(\vec{0},0) \dot{\underline{\underline{\alpha}}}(\vec{s},\tau)\rho_0 \rangle : \underline{\underline{\Phi}}(\vec{r}-\vec{s},t-\tau) + \mathcal{O}(\epsilon^2). \tag{A3}$$

In the present case, $\hat{H}^{(I)}$ is given by Eq. (13), therefore we set $\underline{\underline{\alpha}}=\Sigma_i^N \vec{r}_i\vec{p}_i\delta(\vec{r}_i-\vec{r})$ and $\underline{\underline{\Phi}}=[\vec{\nabla}\vec{u}(\vec{r},t)]^T$.

We have to calculate the velocity field $\vec{v}$ for the system subjected to the perturbation. By following the Irving-Kirkwood theory, we can identify this field by exploiting the equation:

$$\vec{J}^m(\vec{r},t) = m(\vec{r},t)\vec{v}(\vec{r},t) = \langle \vec{g}(\vec{r}) \rangle_t,$$

where we have introduced the flux of momentum $\vec{J}^m$ and the corresponding dynamical variable $\vec{g}$:

$$\vec{g}(\vec{r}) = \sum_i^N m\dot{\vec{r}}_i \delta(\vec{r}_i - \vec{r}). \tag{A4}$$

Expanding the last expression in series of the small parameter ϵ, we find:

$$\vec{v}(\vec{r},t) = \frac{\vec{J}^m(\vec{r},t)}{m(\vec{r},t)} = \frac{\vec{J}_m^{(I)}(\vec{r},t) + \mathcal{O}(\epsilon^2)}{m^{(0)}(\vec{r},t) + m^{(I)}(\vec{r},t) + \mathcal{O}(\epsilon^2)}$$

$$= \frac{V}{mN}\vec{J}_m^{(I)}(\vec{r},t) + \mathcal{O}(\epsilon^2),$$

where we have assumed that in the limit $\epsilon \to 0$: $\vec{J}^m(\vec{r},t) \to 0$ and $m(\vec{r},t) \to \frac{mN}{V}$. Now, by applying the linear response theory Eq. (A3), we find the following equation for the α component of the field $\vec{v}$:

$$v_\alpha(\vec{r},t) = -\frac{V}{mN}\beta \int_0^\infty d\tau \int_V d\vec{s} \langle g_\alpha(\vec{0},0)\dot{\alpha}_{\mu\nu}(\vec{s},\tau)\rangle_0$$

$$\times \nabla_\mu u_\nu(\vec{r}+\vec{s}, t-\tau) + \mathcal{O}(\epsilon^2).$$

Finally, by performing an integration by parts we obtain

$$v_\alpha(\vec{r},t) = \frac{V}{mN}\beta \int_0^\infty d\tau \int_V d\vec{s} \langle g_\alpha(\vec{0},0)\nabla_\mu \dot{\alpha}_{\mu\nu}(\vec{s},\tau)\rangle_0$$

$$\times u_\nu(\vec{r}-\vec{s}, t-\tau) + \mathcal{O}(\epsilon^2),$$

which is a convolution in space and time. Its Fourier transform is

$$\tilde{v}_\alpha(\vec{k},\omega) = \sigma_{\alpha\beta}(\vec{k},\omega)\tilde{u}_\beta(\vec{k},\omega), \tag{A5}$$

where

$$\sigma_{\alpha\beta}(\vec{k},\omega) = \frac{V}{mN}\beta \int_0^{+\infty} d\tau \int d\vec{s} e^{i(-\vec{k}\cdot\vec{s}+\omega\tau)}$$

$$\times \langle g_\alpha(\vec{0},0)\nabla_\mu \dot{\alpha}_{\mu\beta}(\vec{s},\tau)\rangle_0$$

$$= -\frac{V}{mN}\beta \int_0^{+\infty} d\tau e^{i\omega\tau} \langle g_\alpha(\vec{0},0)\widetilde{(\nabla_\mu \dot{\alpha}_{\mu\beta})}(\vec{k},\tau)\rangle_0,$$

where we have performed the integral in $d\vec{s}$ in the second last equality.

In order to evaluate $\sigma_{\alpha\beta}(\vec{k},\omega)$, we have to calculate the Fourier transform $\widetilde{(\nabla_\mu \dot{\alpha}_{\mu\beta})}$. In the following equation, we report the result of this calculation that will be demonstrated at the end of this paragraph. In the case with $k \ll a$, where "a" is the mean free path, we will find

$$\widetilde{(\nabla_\mu \dot{\alpha}_{\mu\beta})}(\vec{k},\tau) = -\dot{\tilde{g}}_\beta(\vec{k},t) - ik_\mu \cdot \sum_i^N (i\vec{k}\cdot\hat{\vec{r}}_i)(\vec{r}_i\vec{p}_i)_{\mu\beta} e^{-i\vec{k}\cdot\vec{r}_i}. \tag{A6}$$

With the aid of the last equation, we can determine $\sigma_{\alpha\beta}$, defined in Eq. (A5), in the limit $k \to 0$:

$$\lim_{k\to 0} \sigma_{\alpha\beta}(\vec{k},\omega) = \frac{V}{mN}\beta \int_0^{+\infty} d\tau e^{i\omega\tau} \langle g_\alpha(\vec{0},0)\dot{\tilde{g}}_\beta(\vec{k}=0,\tau)\rangle_0$$

$$= -\frac{V}{mN}\beta \int_0^{+\infty} d\tau i\omega e^{i\omega\tau} \langle g_\alpha(\vec{0},0)\tilde{g}_\beta(\vec{k}=0,\tau)\rangle_0. \tag{A7}$$

The ensemble average $\langle g_\alpha(\vec{0},0)\tilde{g}_\beta(\vec{k}=0,\tau)\rangle_0$ can be calculated as follows:

$$\langle g_\alpha(\vec{r},0)\tilde{g}_\beta(\vec{k}=0,\tau)\rangle_0 = \left\langle g_\alpha(\vec{r},0)\int d\vec{s} g_\beta(\vec{s},\tau)\right\rangle_0$$

$$= \left\langle \sum_i^N m\dot{r}_{i\alpha}\delta(\vec{r}_i - \vec{r}) \sum_j^N m\dot{r}_{j\beta}(\tau)\right\rangle_0,$$

where we have used the definition of $\vec{g}$ given by Eq. (A4). Now, we note that the quantity $\Sigma_j^N m\dot{r}_{j\beta}(\tau)$ corresponds to the total momentum of the system, therefore it is independent of the time. On the other hand, the overall average on the equilibrium ensemble has to be $\vec{r}$ independent as well. Therefore the following relation holds:

$$\langle g_\alpha(\vec{r},0)\tilde{g}_\beta(\vec{k}=0,\tau)\rangle_0 = \frac{1}{V}\int_V d\vec{r} \left\langle \sum_i^N m\dot{r}_{i\alpha}\delta(\vec{r}_i - \vec{r}) \sum_j^N m\dot{r}_{j\beta}\right\rangle_0$$

$$= \frac{1}{V}\left\langle \sum_i^N m\dot{r}_{i\alpha} \sum_j^N m\dot{r}_{j\beta}\right\rangle_0$$

$$= \frac{m}{V}\left\langle \sum_i^N m\dot{r}_{i\alpha}^2\right\rangle_0 \delta_{\alpha\beta} = m\frac{N}{\beta V}\delta_{\alpha\beta}.$$

In the last equality we have also applied the equipartition theorem $\langle m\dot{r}_{i\alpha}^2\rangle_0 = K_b T = \frac{1}{\beta}$. By replacing the last result in Eq. (A7) we finally find:

$$\lim_{k\to 0} \underline{\underline{\sigma}}(\vec{k},\omega) = -\int_0^{+\infty} d\tau i\omega e^{i\omega\tau}\underline{\underline{I}} = -i\omega \int_{-\infty}^{+\infty} d\tau e^{i\omega\tau}\theta(\tau)\underline{\underline{I}}$$

$$= -i\omega\tilde{\theta}\underline{\underline{I}} = \left(\frac{\tilde{d}\theta}{dt}\right)\underline{\underline{I}} = \tilde{\delta}\underline{\underline{I}} = \underline{\underline{I}},$$

where θ stands for the step function. By comparing this relation to Eq. (A5) we obtain the final result $\tilde{\vec{v}}(\vec{0},\omega) = \tilde{\vec{u}}(\vec{0},\omega)$ that proves the correspondence between the field $\vec{u}$ involved in the "Doll's" perturbation and the macroscopic velocity field $\vec{v}$ induced in the system by the perturbation.

In order to complete the paragraph we have to demonstrate equation Eq. (A6). First of all, we calculate the derivative $\dot{\underline{\underline{\alpha}}}$ as follows:

$$\dot{\underline{\underline{\alpha}}}(\vec{r},t) = \sum_i^N (\dot{\hat{r}}_i\vec{p}_i + \hat{r}_i\dot{\vec{p}}_i)\delta(\vec{r}_i - \vec{r}) + \vec{r}_i\vec{p}_i\left(\hat{r}_i \cdot \frac{\partial}{\partial\vec{r}_i}\delta(\vec{r}_i - \vec{r})\right)$$

$$= \sum_i^N \left(m\dot{\hat{r}}_i\hat{r}_i - \vec{r}_i\sum_{j\neq i}^N \frac{\partial\phi(|\vec{r}_{ij}|)}{\partial\vec{r}_i} - \vec{r}_i\vec{p}_i(\hat{r}_i\cdot\vec{\nabla})\right)\delta(\vec{r}_i - \vec{r}),$$

where we have applied the relation $\frac{\partial}{\partial\vec{r}_i}\delta(\vec{r}_i - \vec{r}) = -\vec{\nabla}\delta(\vec{r}_i - \vec{r})$.

Then, we calculate the Fourier transform on the space variable $\vec{r}$:

$$\tilde{\underline{\underline{\dot{\alpha}}}}(\vec{k},t)=\sum_{i}^{N}\left(m\dot{\vec{r}}_i\dot{\vec{r}}_i-\vec{r}_i\sum_{j\neq i}^{N}\frac{\partial\phi(|\vec{r}_{ij}|)}{\partial\vec{r}_i}+i\vec{r}_i\vec{p}_i(\dot{\vec{r}}_i\cdot\vec{k})\right)e^{i\vec{k}\cdot\vec{r}_i}. \tag{A8}$$

By focusing on the former equation term that involves the derivative of the potential, we find:

$$\begin{aligned}
&\sum_{i}^{N}\sum_{j\neq i}^{N}\vec{r}_i\frac{\partial\phi(|\vec{r}_{ij}|)}{\partial\vec{r}_i}e^{i\vec{k}\cdot\vec{r}_i}\\
&=\frac{1}{2}\sum_{i}^{N}\sum_{j\neq i}^{N}\left(\vec{r}_i\frac{\partial\phi(|\vec{r}_{ij}|)}{\partial\vec{r}_i}e^{i\vec{k}\cdot\vec{r}_i}+\vec{r}_j\frac{\partial\phi(|\vec{r}_{ji}|)}{\partial\vec{r}_j}e^{i\vec{k}\cdot\vec{r}_j}\right)\\
&=\frac{1}{2}\sum_{i}^{N}\sum_{j\neq i}^{N}(\vec{r}_ie^{i\vec{k}\cdot\vec{r}_i}-\vec{r}_je^{i\vec{k}\cdot\vec{r}_j})\frac{\partial\phi(|\vec{r}_{ij}|)}{\partial\vec{r}_i}\\
&=\frac{1}{2}\sum_{i}^{N}\sum_{j\neq i}^{N}e^{i\vec{k}\cdot\vec{r}_j}(\vec{r}_ie^{i\vec{k}\cdot\vec{r}_{ij}}-\vec{r}_j)\frac{\partial\phi(|\vec{r}_{ij}|)}{\partial\vec{r}_i}\\
&=\frac{1}{2}\sum_{i}^{N}\sum_{j\neq i}^{N}e^{i\vec{k}\cdot\vec{r}_j}[\vec{r}_{ij}+\vec{r}_i(i\vec{k}\cdot\vec{r}_{ij}+\mathcal{O}(\vec{k}\cdot\vec{r}_{ij}{}^2))]\frac{\partial\phi(|\vec{r}_{ij}|)}{\partial\vec{r}_i}.
\end{aligned}$$

By means of this result and under the hypothesis of small wave vector limit $ka\ll 1$, Eq. (A8) can be written as follows:

$$\begin{aligned}
\tilde{\underline{\underline{\dot{\alpha}}}}(\vec{k},t)=&\sum_{i}^{N}m\dot{\vec{r}}_i\dot{\vec{r}}_ie^{i\vec{k}\cdot\vec{r}_i}-\frac{1}{2}\sum_{j\neq i}^{N}e^{i\vec{k}\cdot\vec{r}_j}\vec{r}_{ij}\frac{\partial\phi(|\vec{r}_{ij}|)}{\partial\vec{r}_i}\\
&+\sum_{i}^{N}(i\vec{k}\cdot\dot{\vec{r}}_i)(\vec{r}_i\vec{p}_i)e^{i\vec{k}\cdot\vec{r}_i}.
\end{aligned} \tag{A9}$$

Equation (A9) implies that the Fourier transform of the gradient of $\dot{\underline{\underline{\alpha}}}$ fulfills the following equation:

$$\begin{aligned}
&(\vec{\nabla}\cdot\tilde{\underline{\underline{\dot{\alpha}}}})(\vec{k},\tau)\\
&=\left[-i\vec{k}\cdot\left(\sum_{i}^{N}m\dot{\vec{r}}_i\dot{\vec{r}}_ie^{i\vec{k}\cdot\vec{r}_i}-\frac{1}{2}\sum_{j\neq i}^{N}e^{i\vec{k}\cdot\vec{r}_j}\vec{r}_{ij}\frac{\partial\phi(|\vec{r}_{ij}|)}{\partial\vec{r}_i}\right)\right]\\
&\quad-i\vec{k}\cdot\sum_{i}^{N}(i\vec{k}\cdot\dot{\vec{r}}_i)(\vec{r}_i\vec{p}_i)e^{i\vec{k}\cdot\vec{r}_i}.
\end{aligned}$$

This result corresponds to the required Eq. (A6) providing that the quantity in square brackets is equal to $-\tilde{\dot{\vec{g}}}(\vec{k},t)$. This can be easily verified as follows:

$$\begin{aligned}
\tilde{\dot{\vec{g}}}(\vec{k},t)&=\frac{d}{dt}\sum_{i=1}^{N}m\dot{\vec{r}}_ie^{i\vec{k}\cdot\vec{r}_i}=\sum_{i=1}^{N}[m\dot{\vec{r}}_i(i\vec{k}\cdot\dot{\vec{r}}_i)+m\ddot{\vec{r}}_i]e^{i\vec{k}\cdot\vec{r}_i}\\
&=\sum_{i=1}^{N}\left(m\ddot{\vec{r}}_i(i\vec{k}\cdot\vec{r}_i)-\sum_{j\neq i}^{N}\frac{\partial\phi(|\vec{r}_{ij}|)}{\partial\vec{r}_i}\right)e^{i\vec{k}\cdot\vec{r}_i}\\
&=\sum_{i=1}^{N}i\vec{r}\cdot(m\dot{\vec{r}}_i\dot{\vec{r}}_i)e^{i\vec{k}\cdot\vec{r}_i}\\
&\quad-\frac{1}{2}\sum_{i=1}^{N}\sum_{j\neq i}^{N}\left(\frac{\partial\phi(|\vec{r}_{ij}|)}{\partial\vec{r}_i}e^{i\vec{k}\cdot\vec{r}_i}+\frac{\partial\phi(|\vec{r}_{ji}|)}{\partial\vec{r}_j}e^{i\vec{k}\cdot\vec{r}_j}\right)\\
&=\sum_{i=1}^{N}i\vec{k}\cdot(m\dot{\vec{r}}_i\dot{\vec{r}}_i)e^{i\vec{k}\cdot\vec{r}_i}-\frac{1}{2}\sum_{i=1}^{N}\sum_{j\neq i}^{N}\frac{\partial\phi(|\vec{r}_{ij}|)}{\partial\vec{r}_i}(e^{i\vec{k}\cdot\vec{r}_i}-e^{i\vec{k}\cdot\vec{r}_j})\\
&=\sum_{i=1}^{N}i\vec{k}\cdot(m\dot{\vec{r}}_i\dot{\vec{r}}_i)e^{i\vec{k}\cdot\vec{r}_i}-\frac{1}{2}\sum_{i=1}^{N}\sum_{j\neq i}^{N}\frac{\partial\phi(|\vec{r}_{ij}|)}{\partial\vec{r}_i}e^{i\vec{k}\cdot\vec{r}_j}(e^{i\vec{k}\cdot\vec{r}_{ij}}-1)\\
&=\sum_{i=1}^{N}i\vec{k}\cdot(m\dot{\vec{r}}_i\dot{\vec{r}}_i)e^{i\vec{k}\cdot\vec{r}_i}-\frac{1}{2}\sum_{i=1}^{N}\sum_{j\neq i}^{N}\frac{\partial\phi(|\vec{r}_{ij}|)}{\partial\vec{r}_i}\\
&\quad\times e^{i\vec{k}\cdot\vec{r}_j}\{i\vec{k}\cdot\vec{r}_{ij}+\mathcal{O}[(i\vec{k}\cdot\vec{r}_{ij})^2]\}.
\end{aligned}$$

In the limit $ka\ll 1$ we finally get

$$\begin{aligned}
\tilde{\dot{\vec{g}}}(\vec{k},t)&=i\vec{k}\cdot\sum_{i=1}^{N}[m(\dot{\vec{r}}_i\dot{\vec{r}}_i)]e^{i\vec{k}\cdot\vec{r}_i}+\frac{1}{2}\sum_{i=1}^{N}\sum_{j\neq i}^{N}\frac{\partial\phi(|\vec{r}_{ij}|)}{\partial\vec{r}_i}e^{i\vec{k}\cdot\vec{r}_j}(i\vec{k}\cdot\vec{r}_{ij})\\
&=\left[i\vec{k}\cdot\left(\sum_{i=1}^{N}(m\dot{\vec{r}}_i\dot{\vec{r}}_i)e^{i\vec{k}\cdot\vec{r}_i}+\frac{1}{2}\sum_{i=1}^{N}\sum_{j\neq i}^{N}\vec{r}_{ij}\frac{\partial\phi(|\vec{r}_{ij}|)}{\partial\vec{r}_i}e^{i\vec{k}\cdot\vec{r}_j}\right)\right].
\end{aligned}$$

[1] G. Ciccotti and W. G. Hoover, *Molecular Dynamics Simulation of Statistical-Mechanical Systems*, International School of Physics, Course XCVII (North-Holland, Amsterdam, 1986).
[2] M. S. Green, J. Chem. Phys. **19**, 1036 (1951).
[3] R. Kubo, J. Phys. Soc. Jpn. **12**, 570 (1957).
[4] J. P. Hansen and I. R. Mc Donald, *Theory of Simple Liquids*, 3rd ed. (Academic, New York, 2006).
[5] C. Trozzi and G. Ciccotti, Phys. Rev. A **29**, 916 (1984).
[6] A. Tenenbaum, G. Ciccotti, and R. Gallico, Phys. Rev. A **25**, 2778 (1982).
[7] J. Koplik, J. R. Banavar, and J. F. Willemsen, Phys. Rev. Lett. **60**, 1282 (1988).
[8] D. J. Evans and G. P. Morriss, *Statistical Mechanics of Nonequilibrium Liquids* (Academic, London, 1990).
[9] A. W. Lees and S. F. Edwards, J. Phys. C **5**, 1921 (1972).
[10] D. Heyes, J. Chem. Soc., Faraday Trans. 1 **80**, 1363 (1984).
[11] G. Ciccotti and G. Jacucci, Phys. Rev. Lett. **35**, 789 (1975).
[12] G. Ciccotti, G. Jacucci, and I. McDonald, J. Stat. Phys. **21**, 1 (1979).
[13] C. Massobrio and G. Ciccotti, Phys. Rev. A **30**, 3191 (1984).
[14] W. G. Hoover, G. Ciccotti, G. V. Paolini, and C. Massobrio, Phys. Rev. A **32**, 3765 (1985).

[15] G. V. Paolini and G. Ciccotti, Phys. Rev. A **35**, 5156 (1987).
[16] C. Pierleoni, G. Ciccotti, and B. Bernu, Europhys. Lett. **4**, 1115 (1987).
[17] C. Pierleoni and G. Ciccotti, J. Phys.: Condens. Matter **2**, 1315 (1990).
[18] M. N. Honkonnou, C. Pierleoni, and J. P. Ryckaert, J. Chem. Phys. **97**, 9335 (1992).
[19] J. P. Ryckaert, A. Bellemans, G. Ciccotti, and G. V. Paolini, Phys. Rev. A **39**, 259 (1989).
[20] K. Meier, A. Laesecke, and S. Kabelac, J. Chem. Phys. **122**, 014513 (2005).
[21] D. Levesque, L. Verlet, and J. Kurkijarvi, Phys. Rev. A **7**, 1690 (1973).
[22] D. Levesque and L. Verlet, Mol. Phys. **61**, 143 (1987).
[23] M. Schoen and C. Hoheisel, Mol. Phys. **56**, 653 (1985).
[24] C. Hoheisel, J. Chem. Phys. **86**, 2328 (1987).
[25] C. Hoheisel, R. Vogelsang, and M. Schoen, J. Chem. Phys. **87**, 7195 (1987).
[26] W. G. Hoover, D. J. Evans, R. B. Hickman, A. J. C. Ladd, W. T. Ashurst, and B. Moran, Phys. Rev. A **22**, 1690 (1980).
[27] J. H. Irving and J. G. Kirkwood, J. Chem. Phys. **18**, 817 (1950).
[28] H. Mori, Prog. Theor. Phys. **28**, 763 (1962).
[29] D. McQuarry, *Statistical Mechanics* (Harper & Row, New York, 1976).
[30] J. M. Luttinger, Phys. Rev. **135**, 1505 (1964).
[31] G. Ciccotti, C. Pierleoni, and J. P. Ryckaert, in *Microscopic Simulation of Complex Hydrodynamic Phenomena*, edited by M. Mareschal and B. L. Holian (Plenum, New York, 1991).
[32] W. G. Hoover, A. J. C. Ladd, R. B. Hickman, and B. L. Holian, Phys. Rev. A **21**, 1756 (1980).
[33] J. P. Ryckaert, Ber. Bunsenges. Phys. Chem. **94**, 256 (1990).
[34] J. P. Ryckaert, A. Bellemans, G. Ciccotti, and G. V. Paolini, Phys. Rev. Lett. **60**, 128 (1988).
[35] M. Ferrario, G. Ciccotti, B. L. Holian, and J. P. Ryckaert, Phys. Rev. A **44**, 6936 (1991).
[36] C. Pierleoni and J. P. Ryckaert, Phys. Rev. A **44**, 5314 (1991).